Brain Structure and Function (2019) 224:521–532
https://doi.org/10.1007/s00429-018-1782-2

ORIGINAL ARTICLE

A possible postsynaptic role for SNAP-25 in hippocampal synapses

S. Hussain[1] · H. Ringsevjen[1] · M. Schupp[3] · Ø. Hvalby[2] · J. B. Sørensen[3] · V. Jensen[2] · S. Davanger[1,4]

Received: 26 April 2018 / Accepted: 19 October 2018 / Published online: 30 October 2018

Abstract
The SNARE protein SNAP-25 is well documented as regulator of presynaptic vesicle exocytosis. Increasing evidence suggests roles for SNARE proteins in postsynaptic trafficking of glutamate receptors as a basic mechanism in synaptic plasticity. Despite these indications, detailed quantitative subsynaptic localization studies of SNAP-25 have never been performed. Here, we provide novel electron microscopic data of SNAP-25 localization in postsynaptic spines. In addition to its expected presynaptic localization, we show that the protein is also present in the postsynaptic density (PSD), the postsynaptic lateral membrane and on small vesicles in the postsynaptic cytoplasm. We further investigated possible changes in synaptic SNAP-25 protein expression after hippocampal long-term potentiation (LTP). Quantitative analysis of immunogold-labeled electron microscopy sections did not show statistically significant changes of SNAP-25 gold particle densities 1 h after LTP induction, indicating that local trafficking of SNAP-25 does not play a role in the early phases of LTP. However, the strong expression of SNAP-25 in postsynaptic plasma membranes suggests a function of the protein in postsynaptic vesicle exocytosis and a possible role in hippocampal synaptic plasticity.

Keywords SNARE proteins · Electron microscopy · LTP · Synaptic plasticity · Hippocampus

Introduction

Synaptic plasticity is crucial for the ability of the brain to change and adapt to new information. There are many indications that synaptic plasticity is the basis for learning and memory at the cellular and molecular levels (Stuchlik 2014). LTP is an activity-dependent, persistent enhancement of synaptic strength and is a well-characterized form of synaptic plasticity (Bliss and Lomo 1973). Increasing concentrations of postsynaptic glutamate receptors are one of the underlying mechanisms of LTP in the hippocampus (Malinow and Malenka 2002). How these glutamate receptors are inserted postsynaptically by exocytosis is poorly understood.

SNARE proteins mediate intracellular membrane fusion events (Chen and Scheller 2001). In nerve terminals, a SNARE core complex consisting of VAMP2, SNAP-25 and syntaxin-1 is known to be essential for vesicle exocytosis and thereby for synaptic transmission (Hussain and Davanger 2011). SNAP-25 belongs to a family of evolutionarily conserved proteins essential for exocytosis (Risinger et al. 1993). The protein exists in two isoforms that differ by only nine amino acids and are referred to as SNAP-25A and SNAP-25B (Bark and Wilson 1994). An additional member, SNAP-23, which is expressed in all tissues, is 59% identical to SNAP-25 and, similarly to neuronal SNAP-25, it interacts with multiple syntaxins and VAMPs (Ravichandran et al. 1996). SNAP- 29 and SNAP-47 are other isoforms of SNAREs that are ubiquitously expressed in mammals (Hohenstein and Roche 2001; Holt et al. 2006).

SNAP-25 is present in particular subsets of neurons and is located on the cytoplasmic face of the plasma membrane in presynaptic terminals and throughout the axon (Tao-Cheng et al. 2000). Outside the nervous system, SNAP-25 has been detected in pancreatic endocrine cells, secretory anterior pituitary cells, and in other tissues (Sadoul et al. 1995).

✉ S. Davanger
svend.davanger@medisin.uio.no

1 Division of Anatomy, Department of Molecular Medicine, Institute of Basic Medical Sciences, University of Oslo, Oslo, Norway

2 Division of Physiology, Department of Molecular Medicine, Institute of Basic Medical Sciences, University of Oslo, Oslo, Norway

3 Department of Neuroscience, Faculty of Health and Medical Sciences, University of Copenhagen, Copenhagen, Denmark

4 Laboratory of Synaptic Plasticity, Division of Anatomy, Institute of Basic Medical Sciences, P.O.Box 1105, Blindern, 0317 Oslo, Norway

SNAP-25 is well established as part of the fusion machinery in presynaptic exocytosis of neurotransmitters. Increasing evidence indicates a role of SNAP-25 also in postsynaptic trafficking of glutamate receptors and LTP (Gu and Huganir 2016; Selak et al. 2009; Lau et al. 2010; Jurado et al. 2013). Despite indications pointing to postsynaptic functions of SNAP-25, a clear localization of the protein at ultrastructural level in dendritic spines is still lacking. The objective of the present study is to determine differences in SNAP-25 densities in subregions of the synapse and to further analyze possible changes in hippocampal SNAP-25 expression in early phases of LTP.

Materials and methods

Antibodies

Anti-SNAP-25 was raised in rabbit immunized with recombinant SNAP-25 protein (nucleotide: 209-829) fixed in 1.25% glutaraldehyde and mixed with Freund's adjuvant. The SNAP-25 construct (pGEX-KG vector) was a generous gift from Richard Scheller. Crude antiserum was affinity-purified with recombinant glutaraldehyde fixed SNAP-25 protein (affi-gel column).

Primary antibodies

Anti-SNAP-25 (In-house) was used at 1:10,000 for Western blot (WB), 1:40-1:100 for postembedding electron microscopy (EM), 1:100 for light microscopy (LM) and 1:100 for immunofluorescence confocal microscopy (ICM). Anti-TUJ 1 (Covance, CA, USA, Cat# MMS-435P) was used at 1:100, anti-synaptophysin (Abcam, Cambridge, UK, Cat#ab180008) at 1:100 and anti-PSD-95 (Novus Biologics, ON, Canada, Cat#NB300-556) at 1:100 for ICM.

Secondary antibodies

Donkey anti-rabbit Cy3 (Jackson Immuno, MD, USA, Cat#711-165-152) and donkey anti-mouse A488 (Invitrogen, CA, USA, Cat#A21202) were used at 1:1000 for ICM. Mouse anti-rabbit alkaline phosphatase (Sigma, MO, USA, Cat#A3687) was used at 1:10 000 for WB. IgG coupled to 10 nm colloidal gold (British BioCell International, Cardiff, UK, Cat#R14007) was used at 1:20 for EM. Biotinylated goat anti-rabbit (Abcam, Cambridge, UK, Cat#Ab64256) was used at 1:100 for LM, together with streptavidin biotinylated horseradish peroxidase complex (GE healthcare, Buckinghamshire, UK, Cat#RPN1051V) at 1:100.

Animals

Wistar male rats weighing 250–300 g were used for the EM experiments, 1–4 day old Wistar rats of either sex for the primary hippocampal cultures, PVG male rats weighing 200–250 g for WB and the LM study. Experimental protocols were approved by the Institutional Animal Care and Use Committee and conform to National Institutes of Health guidelines for the care and use of animals, as well as international laws on protection of laboratory animals, with the approval of a local bioethical committee and under the supervision of a veterinary commission for animal care and comfort of the University of Oslo. The animals were treated in accordance with the guidelines of the Norwegian Committees on Animal Experimentation (Norwegian Animal Welfare Act and European Communities Council, Directive of 24 November 1986-86/609/EEC). Every effort was made to minimize the number of animals used and their sufferings.

Generation of SNAP-25 knockout embryos (Washbourne et al. 2002): Since the knockout animals are not viable, the heterozygous animals were crossed to generate knockout mice. The mother was killed by cervical dislocation around embryonic day 18 (plus/minus 1 day), followed by Caesarian section to recover knockouts, heterozygotes and wildtype animals. Embryos were killed by decapitation. Left and right hippocampi were dissected from embryonic day 18 (E18) SNAP25-null mutant (–/–) mice and control littermates (+/+) of either sex in HBSS (Sigma), buffered with 7 mM HEPES, and collected in fixative solution (0.1% glutaraldehyde, 4.0% formaldehyde in 0.1 M sodium phosphate buffer). After genotyping, brains from SNAP-25 null mutant (–/–) and control littermates (+/+) were retained. The mice were kept in an Association for Assessment and Accreditation of Laboratory Animal Care (AAALAC)-accredited stable at the Panum Institute, University of Copenhagen and all required permissions were obtained from the Danish Animal Health Inspectorate. The Institutional Animal Care and Use Committee (IACUC) oversaw the procedures.

Immunoblotting

Brain regions of interest were dissected and homogenized. WB analysis was performed using Criterion Cell and Criterion Blotter system (BioRad, CA, USA). Equal amounts of the protein were loaded on Criterion 4–20% pre-cast gel (BioRad), separated by electrophoresis at 200 V for 50 min and electroblotted onto PVDF membrane (Hoefer Scientific Instruments, CA, USA) at 100 V for 60 min. The membranes were blocked with 5% non-fat dried

milk powder in tris-buffered saline with 0.05% Tween-20 (TBST) for 60 min and incubated with primary antibodies and 2.5% non-fat dried milk powder in TBST at room temperature (RT), overnight (ON). The membranes were washed three times for 10 min in TBST and then incubated for 1 h with alkaline–phosphatase linked secondary antibodies and 1.25% non-fat dried milk powder in TBST. The membranes were washed three times for 10 min in TBST. Signals were detected using ECF substrate (Amersham Biosciences, UK) according to the manufacturer's protocol. The membranes were scanned using a fluorescence digital camera detection system (Typhoon and Kodak scanner).

Bright field microscopic studies

Free floating vibratome sections from rat brain (50 µm) were treated with 1.0 M ethanolamine-HCL in 0.1 M sodium phosphate buffer (NaPi), pH 7.4 for 30 min. After washing 3 times × 1 min, the sections were incubated in blocking buffer solution (BB), 10% normal goat serum in NaPi for 1 h and then incubated with primary antibody in BB ON/RT. Next day, the sections were rinsed in NaPi, 3 times x 5 min and BB for 20 min. The sections were then incubated in biotinylated secondary antibody diluted in BB for 1 h at RT and washed 3 times × 5 min with NaPi. The sections were further incubated with streptavidin-biotinylated horseradish peroxidase diluted in BB for 1 h and washed in NaPi 5 times × 10 min. Finally, the sections were incubated in 0.05% diaminobenzidine (DAB) in NaPi for 5 min, before 0.01% H_2O_2 and 0.05% DAB diluted in NaPi for 6 min, before final washing in NaPi 3 times × 5 min. The sections were mounted on microscope slides with heated glycerol gelatin and covered with cover slides.

Preparation of hippocampal neuronal cultures

Primary hippocampal cultures containing both neurons and glial cells of 1–4 day old rats (Wistar) were prepared as previously described (Hasegawa et al. 2004). The cultures were maintained in cell medium Gibcos MEM with the addition of 30 mg/100 ml glutamine; 2,5 mg/100 ml insulin; 5–10% fetal calf serum; 2 ml/100 ml B-27 and 2–10 µl/100 ml ARA-C in 5% CO_2, 95% air incubator at 37 °C. The cultures were used for experiments after 14–21 days. The cultures were labeled with primary antibody in 2% (v/v) normal goat serum, 1% (w/v) bovine serum albumin and 0.4% saponin in NaPi (ON/RT). The cultures were rinsed in NaPi, incubated for 30 min with secondary antibodies at RT and rinsed again in NaPi. Coverslips with cultures were mounted with fluormont mounting media (Southern Biotech), and examined with an Axioplan 2 equipped with a LSM 5 Pascal scanner head (Carl Zeiss, Heidelberg, Germany).

Tetanic stimulation—induction of LTP

Two four-day-old rats were decapitated. Left and right hippocampi were dissected. Transverse slices of 400 µm were cut from the central region of the hippocampi. The slices were placed in a humidified interface chamber and perfused with artificial cerebrospinal fluid (ACSF, 4 °C, bubbled with 95% O_2 – 5% CO_2) containing (in mM): 124 NaCl, 2 KCl, 1.25 KH_2PO_4, 2 $MgSO_4$, 1 $CaCl_2$, 26 $NaHCO_3$ and 12 glucose. Three slices were used as control. Three slices were tetanized in the stratum radiatum pathway. Electrical stimuli were delivered through two tungsten electrodes placed in the proximal and distal stratum radiatum of the CA1 region. Synaptic responses were monitored by two ACSF-filled glass electrodes placed in the corresponding synaptic layers. A high-frequency stimulation protocol was used in the experiments. 100 Hz tetanizations of 1 s durations were delivered eight times with 10 s interval, alternating between the two stimulation electrodes. The current used in these experiments was in the range of 180–800 µA. Synaptic field excitatory post-synaptic potential (fEPSP) responses were monitored before and after the tetanization procedure. The slices were fixed with 4.0% formaldehyde and 1.25% glutaraldehyde 1 h post tetani for the SNAP-25 experiments. The slices were embedded with freeze substitution (see below).

Immersion fixation of SNAP-25 KO and wild-type (WT) mice

Embryos were killed by decapitation. Left and right hippocampi were dissected and immersed in fixative solution (0.1% glutaraldehyde and 4.0% formaldehyde in 0.1 M sodium phosphate buffer). We used immersion fixation of new-born SNAP-25 KO mice since these animals die immediately after birth. Hippocampi from three KO and three WT mice were embedded with freeze substitution (see below).

Perfusion fixation of the rats

Three rats were deeply anesthetized with Equithesin (0.4 ml/100 g body weight) followed by intracardiac perfusion initiated with a 10–15 s flush of 4% Dextran-T70 in NaPi followed by a mixture of 4.0% formaldehyde and 0.1% glutaraldehyde in the same buffer (0.5 l). Each rat was perfused with 500 ml fixative over 15–20 min. The rats were then left ON in a cold room. The next day, the brains were carefully dissected out and stored in NaPi with a mixture of 0.4% FA and 0.01% GA. From each animal, six small (0.5–1.0 mm) blocks from the CA1 region of the hippocampus were dissected and freeze substituted (see below).

Freeze substitution

The tissue blocks were cryoprotected in increasing concentrations of glycerol (30 min in 10%, 30 min in 20%, and overnight in 30% at 4 °C) in 0.1 M phosphate buffer and then frozen in a cryofixation unit (Reichert KF80, Vienna, Austria) filled with propane which was cooled down by liquid nitrogen. Afterwards, the tissue was transferred to 1.5% uranyl acetate diluted in anhydrous methanol into the pre-cooled chamber (− 90 °C, ON). The tissue pieces were placed in Reichert capsules in a flow-through chamber filled with 1.5% uranyl acetate diluted in anhydrous methanol in a pre-cooled chamber (− 90 °C) in a Reichert Automatic Freeze-Substitution unit (AFS) (Leica, Germany). Following 30 h in − 90 °C, the temperature was raised with 4 °C increments per hour from − 90 to − 45 °C. The tissue pieces were then rinsed with anhydrous methanol and infiltrated with Lowicryl HM20 resin (Polysciences, Inc., Warrington, PA 18976, Cat#15924). Infiltration in 1:1 and 2:1 methanol to pure Lowicryl lasted for 2 h each, and 2 h in pure Lowicryl, before ON in pure Lowicryl. The Reichert capsules were moved to Lowicryl-filled gelatin capsules and then transferred to another container filled with ethanol. The resin/tissue was polymerized with UV-light for 24 h, still at − 45 °C. The temperature was increased by 5 °C increments to a final 0 °C where it was polymerized for further 35 h. Ultra-thin sections (90 nm) were cut with a diamond knife (Diatome ultra 45°, Diatome, US) on an ultramicrotome (Reichert Ultracut S-2.GA-E-12/92, Leica Microsystems, Germany) and placed on coated (Coat-Quick "G") nickel grids (Electron Microscopy Sciences, G300-Ni).

Quantitative postembedding Immunocytochemistry

Quantitative analysis of SNAP-25 immunogold labeling in the subregions of the synapse: Semithin sections of the blocks were cut to identify the stratum radiatum region with the LM. From each animal, one block with the best ultrastructure was selected. Three ultrathin sections from each animal/block were immunolabeled essentially as described previously (Mathiisen et al. 2006). 20 synaptic profiles from each section with clearly visible pre- and post-synaptic plasma membranes and vesicles membranes were selected from each section for quantitative analysis. Similar selections were made for dendritic profiles in separate images. A total of 180 images of synapses and 180 images of dendrites were used. From each image of a synapse, we examined six ROIs, and from each image of a dendrite we examined two ROIs, giving a total of 1440 ROIs quantified.

Hippocampal slices induced with LTP: three ultrathin sections from each slice in LTP and control group were immunolabeled. 20 synaptic profiles from each section were used for quantification. A total of 180 profiles were quantified in each group, 360 profiles in total.

SNAP-25 KO and WT mice: two blocks with the best ultrastructure from each group were selected. Two ultrathin sections from each animal/block were immunolabeled. Five synaptic profiles from each section were used for quantification. A total 20 profiles were quantified in each group.

Pre-incubation experiments: Rat brain with the best ultrastructure was selected for immunolabeling with anti-SNAP-25 antibody after pre-incubation with the same antigen used for immunization of the rabbits. Two sections from the pre-incubation group and two sections from the control group were immunolabeled. Ten synaptic profiles from each section were quantified. A total of 20 profiles were quantified in each group.

EM quantification and statistical analysis: The sections were examined with Philips Fei Tecnai 12 electron microscope at 60 kV. Electron micrographs were obtained at random from the middle layer of stratum radiatum of the CA1 region of the hippocampus. SNAP-25 immunolabeling was quantified as number of gold particles/µm of membrane length in asymmetric synapses and as number of gold particles/μm^2 for region of interests in the corresponding intracellular compartments. Specific ROIs were defined and used for quantifications: The postsynaptic density (PSD); the active zone (AZ); the lateral synaptic membranes, i.e., on each side of the PSD (PoL) or the AZ (PreL); the postsynaptic cytoplasm (PoCy); the presynaptic cytoplasm (PreCy); the dendritic membrane (DM); the dendrite cytoplasm (DCy). The synaptic lateral membranes were defined for convenience of measurement as equal to the length of the PSD, on both sides of the PSD or the AZ, for all synapses. SNAP-25 immunogold labeling in the sections from SNAP-25 KO mice and preincubation experiment was quantified over the AZ. An in-house extension to analySIS connected with SPSS (SPSS Inc, Chicago, IL, USA) was used to evaluate the gold particle labeling of the ROIs. The software calculated area particle density (number per unit area) over cytoplasmic compartments and linear particle density (number per unit length of curve) over membrane domains. In the latter case, it measured the distance from each particle-centre to the membrane and included only those particles, which were within an operator-defined distance from the curve segment. For general plasma membranes, the inclusion distance was symmetric between + 21 nm and − 21 nm (negative values signifying an intracellular location). Data for particles were collected in ASCII files as flat tables and exported to SPSS for further statistical and graphical analysis. ImageJ was used to calculate the diameter of SNAP-25 labeled postsynaptic vesicles. Six sections from two blocks/animals were immunolabeled. Ten images from each section were used for the analysis. One postsynaptic vesicle was selected from

each image. A total of 60 labeled postsynaptic vesicles were analysed.

Results

Specificity of in-house antibody

In the present study, we used a SNAP-25 antibody that we raised against a peptide antigen pretreated with glutaraldehyde. To ensure specificity of our in-house antibody, we performed postembedding immunogold labeling of the hippocampus from newborn SNAP-25 KO mice. Quantitative analysis showed 82% reduction of gold particle density over the AZ in the KO (1.8 ± 0.75) compared to the WT (10.1 ± 1.9) animals (Fig. 1a). The difference in labeling intensity was significant ($n = 20$ in both groups; p value < 0.001, Mann–Whitney test). We further performed immunogold labeling of the hippocampus from adult rat with in-house SNAP-25 antibody after pre-incubation with the same antigen used for immunization of rabbits. Quantification of gold particles over the AZ showed a 95% reduction in the pre-incubation group (0.8 ± 0.5) compared to the control group (18.2 ± 2.5) (Fig. 1b). The reduction of labeling intensity between the groups was significant ($n = 20$ in both groups; p value < 0.001, Mann–Whitney test).

Expression of SNAP-25 in the brain

Quantitative WB analysis of whole brain homogenate revealed the highest concentrations of SNAP-25 in the hippocampus and thalamus (Fig. 2a, b). The lowest levels of SNAP-25 among the analyzed brain regions were observed in the cerebellum and spinal cord. The brain stem and cortex showed 89% and 80%, respectively, of SNAP-25 concentration in the hippocampus. We further performed light microscopic investigations of vibratome brain sections to determine the cellular localization of SNAP-25 in different brain regions (Fig. 2c). Immunolabeling of SNAP-25 displayed strong staining of the cortex, hippocampus, thalamus and cerebellum (Fig. 2C1–C3). White matter such as the corpus callosum was only weakly labeled. At the cellular level, somata and proximal dendrites in the CA1 and CA3 regions of the hippocampus showed strong expression of SNAP-25 (Fig. 2C4, C5). The same pattern was observed in thalamic neurons and cortical pyramidal neurons (Fig. 2C6, C7).

SNAP-25 is localized in postsynaptic spines

We conducted ultra-resolution immunogold electron microscopy of SNAP-25 in the CA1 region of the hippocampus to determine the localization of the protein within synapses. SNAP-25 labeling was clearly membrane associated

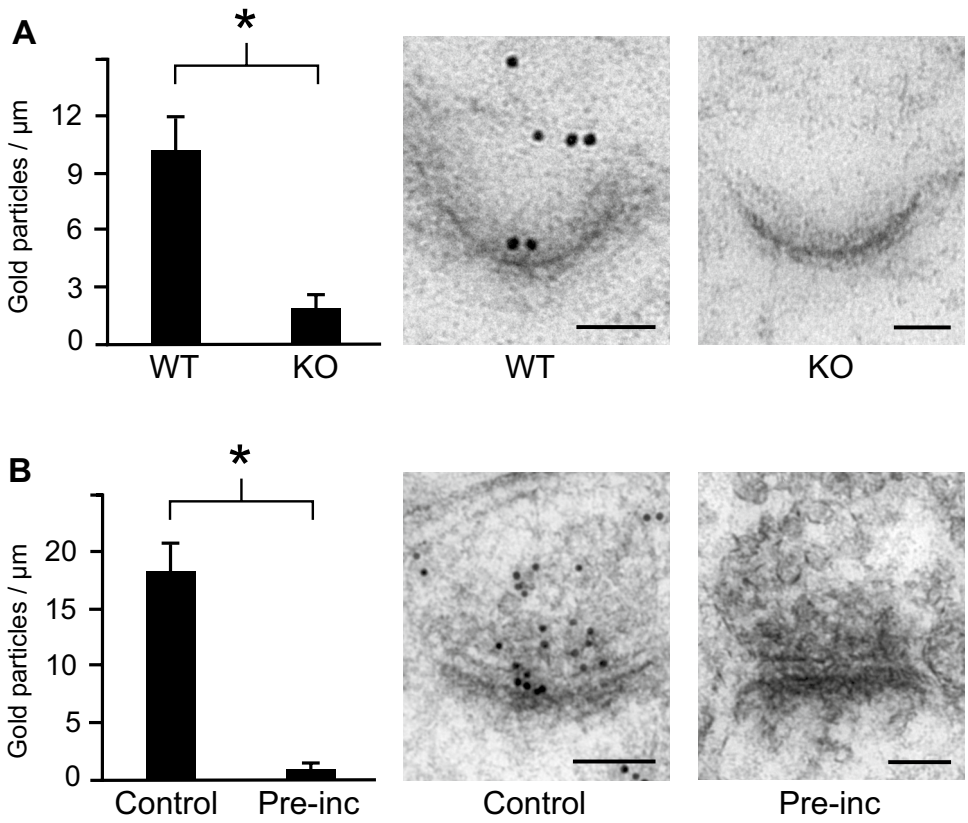

Fig. 1 Specificity controls of in-house SNAP-25 antibody. **a** Electron micrographs and quantitative analysis of SNAP-25 immunogold labeling over the AZ of hippocampal synapses from SNAP-25 KO (95% CI: 1 ± 1.3) and WT mice (95% CI: 10 ± 3.5). **b** Electron micrographs and quantitative analysis of immunogold labeling with SNAP-25 antibody pre-incubated with antigen (95% CI: 0 ± 0.88) or control labeling (95% CI: 18 ± 4.8), over the AZ of hippocampal synapses. Error bars denote SEM. Scale bars **a**, WT, 50 nm; KO, 50 nm. **b** Control, 100 nm; peptide pre-incubation, 50 nm

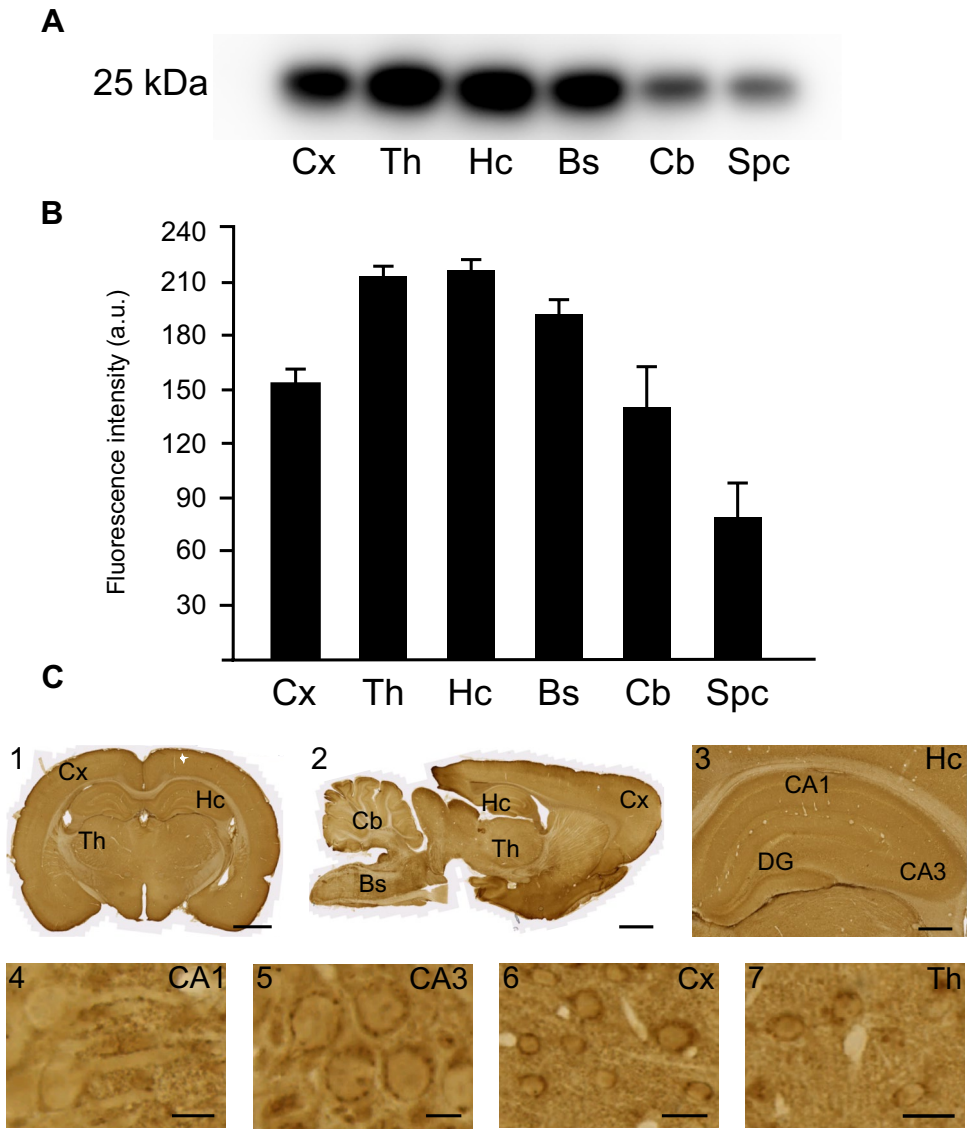

Fig. 2 Quantitative Western blot and immunohistochemistry of different brain regions. **a** WB of homogenates from different brain regions labeled with SNAP-25 antibody, i.e., cortex (Cx), thalamus (Th), hippocampus (Hc), brain stem (Bs), cerebellum (Cb), and spinal cord (SpC). **b** Quantitative analysis of band intensities seen above. Error bars show SEM. **c** DAB immunoperoxidase staining of brain sections with SNAP-25 antibody. (C1–C3) Staining of neurons in the hippocampus, cerebellum, cerebral cortex and thalamus; (C4) CA1; (C5) CA3; (C6) Cortex; (C7) Thalamus. Scale bars: (C1) 1000 µm. (C2) 2000 µm. (C3) 500 µm. (C4, C5) 10 µm. (C6, C7) 25 µm

(Fig. 3c). Most of the presynaptic labeling was found over the AZ (Fig. 3f), as expected. However, some gold particles were also present over presynaptic vesicles. Strikingly, gold particles representing SNAP-25 were also found on postsynaptic spines, exhibiting a similar pattern as in presynaptic terminals, i.e., the PSD showed the highest labeling intensity (Fig. 3g). Gold particles were also located over the spine cytoplasm, often in relation to small postsynaptic vesicles close to the PSD (Fig. 3d). These postsynaptic vesicles had a mean diameter of 23.4 ± 0.4 nm ($n = 60$). Perisynaptic labeling (lateral synaptic) could be seen both pre- and postsynaptically. In dendrites, SNAP-25 was localized over the plasma membrane and associated with cytoplasmic vesicles (Fig. 3e). Double immunofluorescence labeling of SNAP-25 and the presynaptic marker PSD-95 in dissociated hippocampal cultures produced punctate colocalization of the proteins in spines (Fig. 3a), confirming a postsynaptic expression of SNAP-25. The protein was also co-expressed with the presynaptic vesicle protein synaptophysin (Fig. 3b).

SNAP-25 densities in subregions of the synapse

To compare densities of SNAP-25 in different compartments of the synapse, and also to evaluate the degree of postsynaptic SNAP-25 expression relative to presynaptic expression, we quantified the mean number of immunogold particles over the different cytoplasmic and membrane regions shown in Fig. 4a (Haglerød et al. 2009). This enabled us to estimate whether SNAP-25 is present in the dendritic spine in sufficient numbers necessary to play a role in postsynaptic vesicle docking and fusion. Our quantitative analysis showed that SNAP-25 is significantly expressed in postsynaptic spines, though at somewhat lower levels than in the presynaptic terminal. Specifically, the postsynaptic plasma

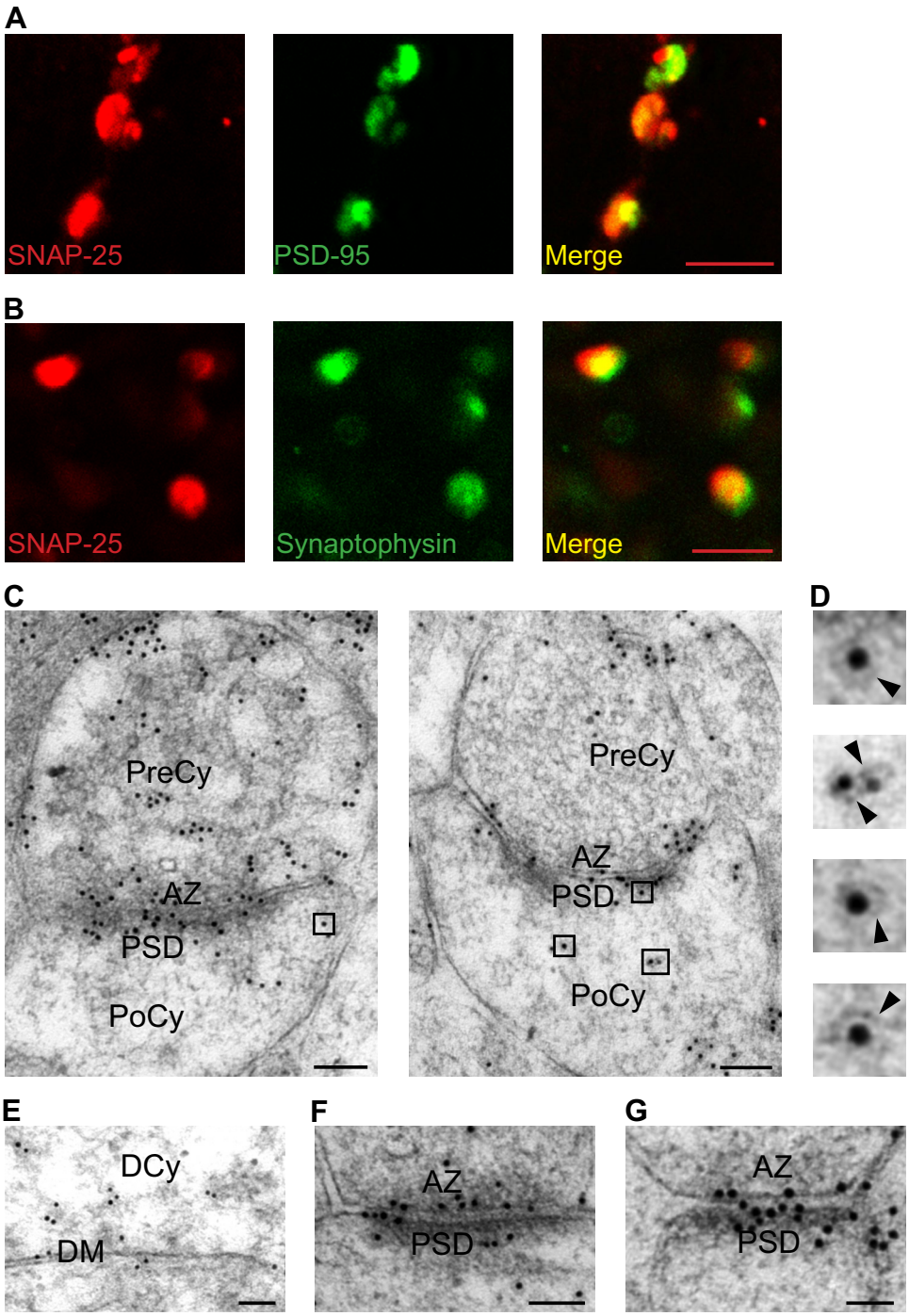

Fig. 3 Electron microscopy of SNAP-25 immunogold labeling in hippocampal asymmetric synapses and double immunofluorescence labeling of SNAP-25 and postsynaptic markers in dissociated hippocampal cultures. **a** Double immunofluorescence staining of dissociated hippocampal cultures with anti-SNAP-25 (red) and anti-PSD-95 (green) showing colocalization of the proteins in synaptic boutons (yellow). **b** Double immunofluorescence staining of dissociated hippocampal cultures with anti-SNAP-25 (red) and anti-synaptophysin (green) showing colocalization of the proteins in synaptic boutons (yellow). **c** Electron micrographs of SNAP-25 immunoreactivity in excitatory synapses from the CA1 region of the rat hippocampus. Selected postsynaptic vesicles are marked with squares. **d** Selected postsynaptic vesicles (arrowheads) at higher magnification. **e** Electron micrograph displaying SNAP-25 immunogold labeling in dendrite. **f** SNAP-25 labeling of AZ at higher magnification. **g** SNAP-25 labeling of PSD at higher magnification. For abbreviations, see legend for Fig. 4. Scale bars: **a, b** 5 µm. **c** 100 nm. **e–g** 50 nm

membrane corresponding to the PSD had a SNAP-25 labeling density of around 50% of the presynaptic AZ, though it was over three times as high as over the dendritic plasma membrane (Fig. 4d). Furthermore, the SNAP-25 membrane expression over the PSD was around 50% more than the immediately adjacent postsynaptic lateral membrane. In the cytoplasmic compartments, the SNAP-25 levels in the postsynaptic spine was around 80% of the presynaptic terminal, but still double the levels in dendritic cytoplasm (Fig. 4c). We also calculated the mean number of immunogold particles in the cytoplasmic compartments as a function of the distance from a line drawn along the middle of the synaptic cleft. This analysis showed that in spite of clearly being present also in the synaptic cytoplasm, the highest densities of SNAP-25 are clearly localized in the immediate vicinity (within 30 nm) to the two synaptic plasma membranes (Fig. 4b), as would be expected of a primarily plasma membrane-associated t-SNARE.

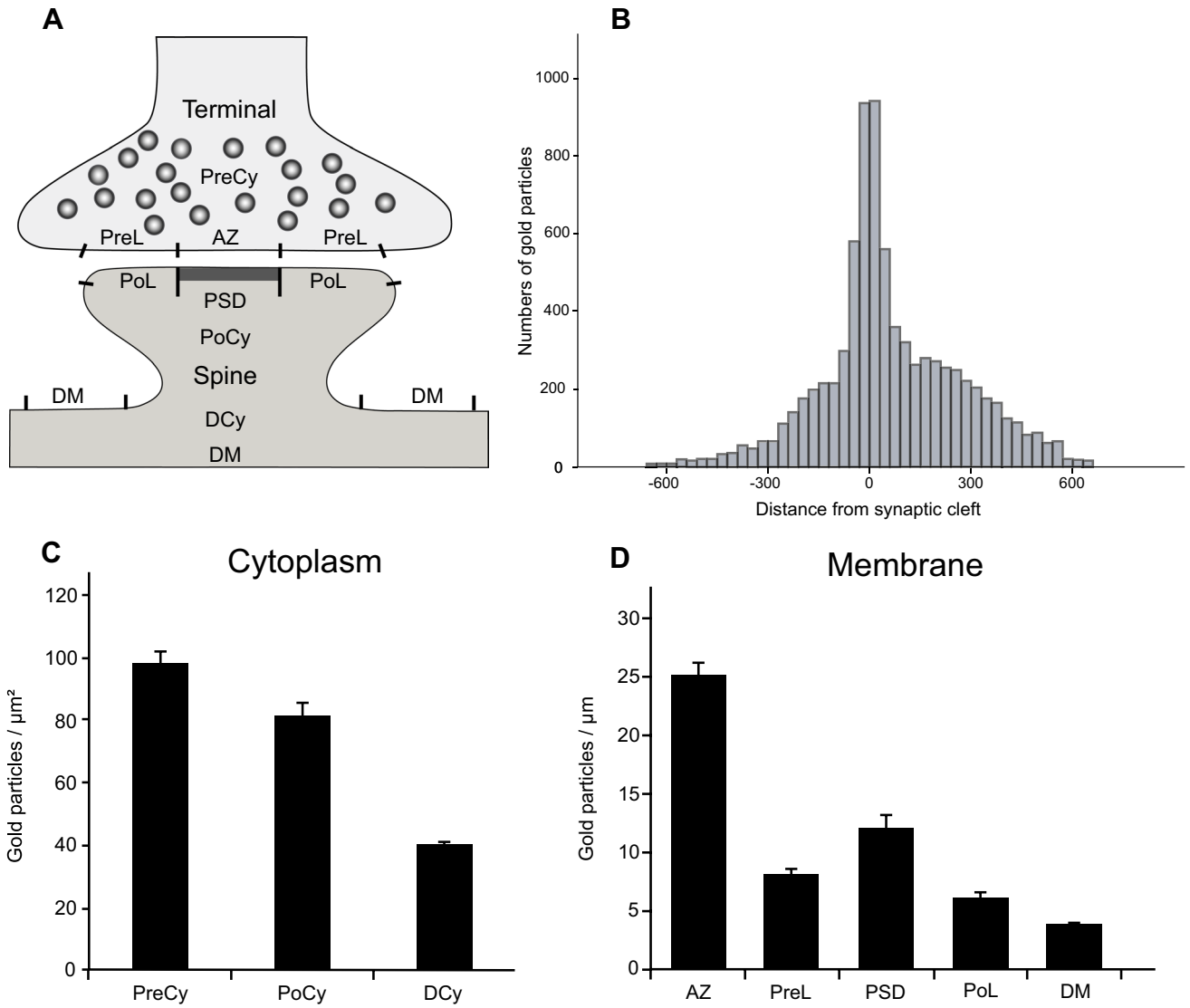

Fig. 4 Quantitative analysis of SNAP-25 immunogold labeling in the subregions of the synapse. **a** Schematic illustration of synaptic regions used for quantitative analysis. The postsynaptic density (PSD); the active zone (AZ); the lateral or perisynaptic membranes, i.e., on each side of the PSD (PoL) or the AZ (PreL); the postsynaptic cytoplasm (PoCy); the presynaptic cytoplasm (PreCy); the dendritic membrane (DM); the dendritic cytoplasm (DCy). **b** Transverse histogram showing the mean numbers of gold particles at every 30 nm from the center of synaptic cleft, negative values are postsynaptic, positive values are presynaptic. **c** Mean SNAP-25 immunogold labeling over cytoplasmic regions of interest. **d** Mean SNAP-25 immunogold labeling over plasma membrane regions of interest. Error bars denote SEM

Slightly reduced synaptic expression of SNAP-25 in hippocampal slices after LTP

We performed quantitative immunogold analysis of ultrathin sections from hippocampal slices to detect possible changes in the synaptic densities of SNAP-25 after induction of hippocampal LTP (Fig. 5a, b). All synaptic membrane regions analyzed, except the postsynaptic lateral membrane, showed reduced levels of SNAP-25 in the LTP group. Presynaptic SNAP-25 immunogold densities at the AZ (Ctrl: 12.9 ± 0.8, LTP: 11.9 ± 0.7) and the PreL (Ctrl: 8.1 ± 0.5, LTP 7.8 ± 0.4) were reduced by 8% and 4%, respectively, in the LTP group compared to the control group (Fig. 5d). In the postsynaptic compartment, analysis revealed a 7% reduction of SNAP-25 density at the PSD (Ctrl: 9.0 ± 0.6, LTP 8.4 ± 0.6) in the LTP group, while the PoL (Ctrl: 4.3 ± 0.4, LTP: 4.5 ± 0.3) showed almost equal levels of SNAP-25 in both groups (Fig. 5e). However, comparing means of linear particle densities between the LTP and the control group by Mann–Whitney test showed no significant differences for any of the regions ($n = 182$ in the control group and $n = 181$ in the experiment group; p values: 0.86 for the AZ; 0.75

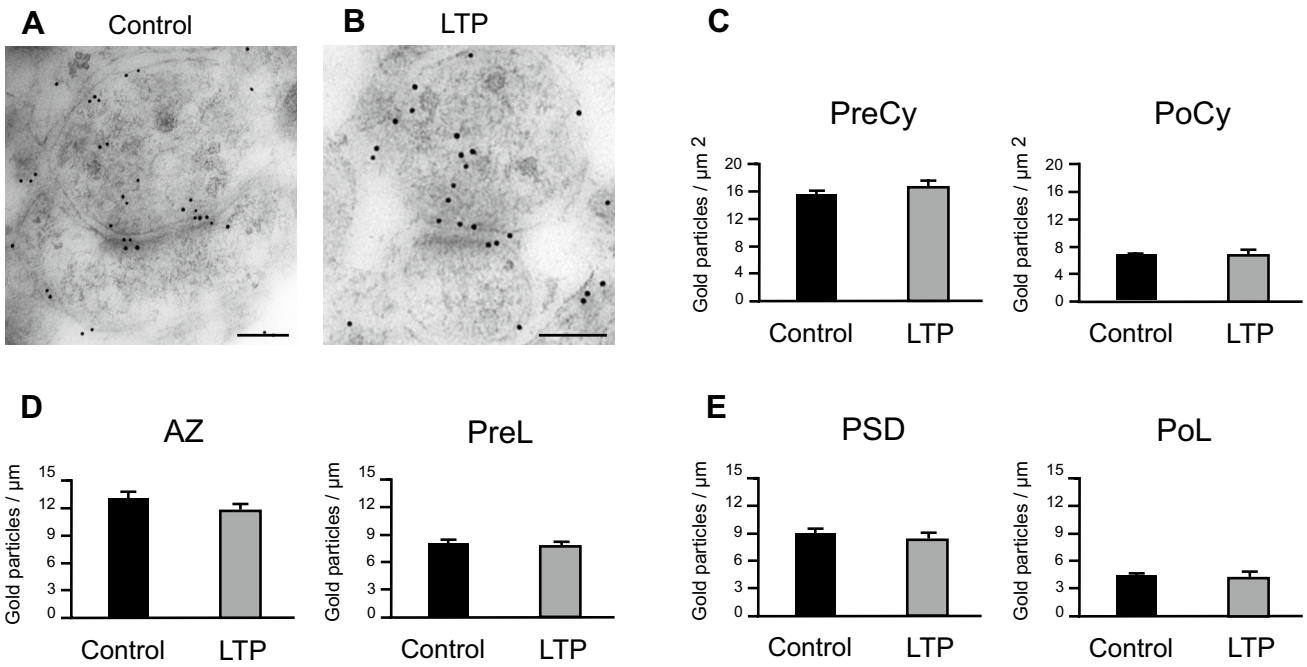

Fig. 5 Electron microscopy and quantitative analysis of SNAP-25 immunogold labeling in hippocampal slices after induction of LTP. **a, b** Electron micrographs showing SNAP-25 immunogold labeling in asymmetric synapses from hippocampal slice induced with LTP and control slice. **c** Mean immunogold labeling over cytoplasmic regions of interest. **d** Mean immunogold labeling over presynaptic membrane regions of interest. **e** Mean immunogold labeling over postsynaptic membrane regions of interest. Error bars denote SEM. Scale bars 150 nm

for the PreL; 0.89 for the PSD; 0.07 for the PoL). Unlike plasma membrane labeling, analyses of cytoplasmic staining showed a slight increase in SNAP-25 in both the pre- and postsynaptic cytoplasm in the LTP group. SNAP-25 labeling in the PreCy (Ctrl: 15.6 ± 0.8, LTP: 16.9 ± 0.9) and the PoCy (Ctrl: 7.0 ± 0.4, LTP: 7.3 ± 0.6) were respectively 8% and 4% higher in the LTP group than in the control group (Fig. 5c). However, these differences did not reach statistical significance ($n = 166$ in the control group and $n = 121$ in the experiment group; p-values: 0.56 for PreCy and 0.31 for PoCy). Thus, in our material, SNAP-25 membrane expression is not significantly changed during the first hour after LTP induction.

Discussion

WB and immunohistochemistry results demonstrated regional variations in SNAP-25 concentrations among the different brain regions. The highest concentration was detected in the hippocampus and the lowest in the spinal cord. This is in line with our previous studies of cognate SNARE proteins VAMP-2 (Hussain and Davanger 2015), syntaxin-1 (Hussain et al. 2016) and SNARE interacting protein synaptotagmin 1 (Hussain et al. 2017). These proteins, together with SNAP-25, constitute the SNARE core complex (Hussain and Davanger 2011), which facilitates vesicle exocytosis. As expected, all these proteins showed a similar distribution pattern in the rat brain.

The present study, to our knowledge, is the first to provide a detailed, quantitative account of SNAP-25 localization in the synapse. Based upon our WB and immunohistochemistry results, we selected the hippocampus for quantitative postembedding immunogold electron microscopy. Our results show that the SNAP-25 plasma membrane expression along the AZ is 70% higher than along the immediately bordering presynaptic lateral membrane. This is consistent with the function of the AZ as specialized zone for vesicle exocytosis. Another study (Hagiwara et al. 2005) did not show significant differences in SNAP-25 density between the AZ and extrasynaptic plasma membrane surrounding the AZ in the synapses. They used dodecyl sulfate-digested freeze-fracture replica labeling and defined AZ by labeling of cytomatrix (CAZ) proteins at the AZ. Extrasynaptic plasma membrane was collected in the same face labeled for CAZ proteins excluding the annulus surrounding the labeled area in a 100-nm width, which may include the AZ. In our work, the synaptic lateral membranes were defined as equal to the length of the PSD, on both sides of the PSD or AZ, for all synapses. Different methods to define the PreL may possibly partly explain the discrepancies in the SNAP-25 levels between AZ and PreL in these two studies. However,

the presence of SNAP-25 along the presynaptic lateral membrane indicates that vesicle fusion occurs also in lateral terminal areas.

In the presynaptic cytoplasm, SNAP-25 was clearly associated with synaptic vesicles. This observation is in agreement with previous studies (Duc and Catsicas 1995; Tao-Cheng et al. 2000; Garbelli et al. 2008; Walch-Solimena et al. 1995). SNAP-25 containing vesicles may either emanate from endocytic recycling, or transport newly synthesized SNAP-25 to the plasma membrane, but there is also evidence that SNAP-25 is a bona fide constituent of synaptic vesicles (Walch-Solimena et al. 1995; Takamori et al. 2006) Mandolesi and coworkers (Mandolesi et al. 2009) did not find SNAP-25 staining in dendrites, while Tao-Cheng (Tao-Cheng et al. 2000) reported that SNAP-25 labeling was seen in the cytoplasm of the large dendrites and excluded from the dendritic membrane. We detected low levels of SNAP-25 in both dendritic cytoplasm and plasma membranes. In the present study, we used in-house SNAP-25 antibodies raised against antigen pretreated with glutaraldehyde to improve immunolabeling at the electron microscopical level. We believe that these antibodies have uncovered localization of SNAP-25 in the brain that has not been demonstrated previously.

There is indirect evidence in the literature for a postsynaptic role of SNAP-25. The protein has been shown to control trafficking of kainate receptors (Selak et al. 2009). In this report, SNAP-25 was associated with GluK5 in biochemically isolated complexes and colocalized in transfected HEK293 cells. In hippocampal slices, SNAP-25 antibodies caused a significant increase in KAR-mediated EPSC.

Another study, (Lau et al. 2010) showed that SNAP-25 is functionally relevant to PKC dependent NMDAR insertion. The authors demonstrated that a SNAP-25 C-terminal blocking peptide suppressed PKC potentiation NMDAR EPSC at CA3 synapses. In the absence of SNAP-25, postsynaptic 'mini' EPSC responses are depressed in amplitude (Tafoya et al. 2006; Bronk et al. 2007; Delgado-Martinez et al. 2007) consistent with an effect on postsynaptic glutamate receptor density. The protein has also been shown to control PSD-95 clustering and spine morphogenesis (Fossati et al. 2015). Despite the evidence indicating a postsynaptic role of SNAP-25, a clear localization of the protein in dendritic spines is still missing. Some studies claim presence of SNAP-25 in postsynaptic terminals using immunofluorescence or ground state depletion microscopy (Selak et al. 2009; Tomasoni et al. 2013). However, the majority of studies have localized SNAP-25 exclusively in the presynaptic compartment through immunogold labeling (Duc and Catsicas 1995; Hagiwara et al. 2005; Mandolesi et al. 2009; Garbelli et al. 2008; Holderith et al. 2012; Kerti et al. 2012). Expression of SNAP-25 in dendritic spines is still a disputed topic.

The mechanisms underlying vesicle exocytosis in the presynaptic terminals of neurons, including neurotransmitter release, have been extensively studied. However, the mechanisms responsible for postsynaptic vesicle trafficking is far less understood. Here, we provide, for the first time, novel electron microscopic data revealing postsynaptic localization of SNAP-25 at hippocampal Schaffer collateral-CA1 synapses. The protein was strongly expressed in dendritic spines at densities lower than in the presynaptic terminal, but still more than in the corresponding dendritic compartment. The densities of SNAP-25 were 50% stronger at the PSD compared to the adjacent lateral membranes. This may indicate more exocytotic activity directly at the PSD compared to other areas of postsynaptic plasma membrane. This is very much in accordance with our previously published data on VAMP2 (Hussain and Davanger 2015), syntaxin 1 (Hussain et al. 2016) and synaptotagmin 1 (Hussain et al. 2017), which are also enriched in the PSD compared to the lateral postsynaptic membranes. Though the prevailing view is that plasma membrane insertion of receptors occurs in perisynaptic regions, our data clearly show that the molecular exocytosis machinery is enriched specifically in the PSD. More functional experiments and colocalization studies with glutamate receptors are necessary to investigate this topic further.

SNAP-25 has been shown to bind the adaptor protein p140Cap in addition to the plasma membrane (Tomasoni et al. 2013). p140Cap plays a role in regulating actin cytoskeleton and spine formation. Our results may thus also provide a basis for a role for SNAP-25 in synaptic plasticity through structural formation and regulation of spines. SNAP-25 was detected in the spine cytoplasm, associated with small postsynaptic vesicles as we have shown previously for VAMP2 (Hussain and Davanger 2015), synataxin-1 (Hussain et al. 2016) and synaptotagmin 1 (Hussain et al. 2017). In our material SNAP-25 labeled postsynaptic vesicles had a mean diameter of 23.4 nm which is about the same as VAMP2 containing postsynaptic vesicles with a mean diameter of 25 nm (Hussain and Davanger 2015).The small postsynaptic vesicles were located close to the PSD and the postsynaptic lateral membrane. Some gold particles were also present deeply within the postsynaptic cytoplasm. SNAP-25 in the spine cytoplasm may be a reserve pool of protein ready to be inserted to the cell membrane in response to increased demand of vesicle exocytosis. These vesicles may also originate from endocytosis or transport newly synthesized SNAP-25 to the plasma membrane. Our findings suggest that SNAP-25 plays a role in the molecular fusion machinery also at the postsynaptic part of the synapse, and may possibly be involved in insertion of glutamate receptors, which is relevant for synaptic plasticity.

Some recent studies indicate a role of SNAP-25 in LTP. Jurado et al. (2013) showed that knockdown of either

SNAP-25 or SNAP-47, but not SNAP-23, impairs LTP in both slices and cultured neurons. The SNAP-25 knockdown decreased NMDAR concentrations at the synapse to a degree that was sufficient to impair LTP induction. These results are in accordance with the work cited above (Lau et al. 2010), which demonstrated that SNAP-25 is functionally relevant to PKC-dependent NMDAR insertion to the cell surface. As far as we know, no studies have examined change of synaptic SNAP-25 concentration during LTP. Having established the presence of SNAP-25 in postsynaptic terminals, we did quantitative analyses of SNAP-25 expression in glutamatergic Schaffer collateral CA1 synapses in the stratum radiatum region one hour after LTP was induced by a high-frequency stimulation protocol. Our hypothesis was that SNAP-25 synaptic expression may differ during the early phases of synaptic plasticity due to its possible role in postsynaptic receptor amplification (Lau et al. 2010). However, our results revealed no significant changes in local SNAP-25 levels in selected regions of interest in the Schaffer collateral-CA1 synapses in this time frame. This may indicate that no distributional changes take place in these regions 1 h post tetanization.

It is, however, also possible that differences in SNAP-25 expression would appear using different time frames. Increased transcription or de novo synthesis would not be detected in our experiments, as this occurs during later phases of LTP (so-called L-LTP). Interestingly, it has previously been reported that mRNA levels of SNAP-25 are increased in granule cells of the dentate gyrus 2 h following LTP induction (250 Hz high-frequency stimulation) of the perforant path (Roberts et al. 1998). There are a vast number of synapses in the stratum radiatum region of CA1, which could make it difficult to detect differences in protein densities after stimulation with the two electrodes used to induce LTP. In fact, each pyramidal cell in CA1 receives 30,000 excitatory inputs (Megias et al. 2001). It is impossible to tell which ones of these were stimulated and potentiated during the electrophysiology experiments. It is also possible that an even larger number of synapses would need to be analyzed to obtain significant results. In spite of our present results, a role of SNAP-25 during synaptic plasticity may very well be possible.

In conclusion, we propose that SNAP-25 is part of the fusion machinery at the postsynaptic membrane, where we for the first time have shown it to be localized, using immunogold electron microscopy. The possible regulation of SNAP-25 during synaptic plasticity needs further investigations.

Acknowledgements We thank Karen Marie Gujord, Jorunn Knutsen, Bjørg Riber, Johannes Helm and Bashir Hakim for their expert technical assistance. We thank Finn-Mogens S. Haug for assistance with immunogold quantification and statistics. The University of Oslo, and the European Union Projects QLG3-CT-2001-02089 (KARTRAP) and LSCHM-CT-2005-005320 (GRIPANNT) supported this work. The authors declare that they have no competing interests.

Compliance with ethical standards

Ethical approval Experimental protocols were approved by the Institutional Animal Care and Use Committee and conform to National Institutes of Health guidelines for the care and use of animals, as well as international laws on protection of laboratory animals, with the approval of a local bioethical committee and under the supervision of a veterinary commission for animal care and comfort of the University of Oslo and the University of Copenhagen. The animals were treated in accordance with the guidelines of the Norwegian Committees and Danish Animal Health Inspectorate on Animal Experimentation (Norwegian/Danish Animal Welfare Act and European Communities Council, Directive of 24 November 1986–86/609/EEC). Every effort was made to minimize the number of animals used and their sufferings. This article does not contain any studies with human participants performed by any of the authors.

References

Bark IC, Wilson MC (1994) Human cDNA clones encoding two different isoforms of the nerve terminal protein SNAP-25. Gene 139(2):291–292

Bliss TV, Lomo T (1973) Long-lasting potentiation of synaptic transmission in the dentate area of the anaesthetized rabbit following stimulation of the perforant path. J Physiol 232(2):331–356

Bronk P, Deak F, Wilson MC, Liu X, Sudhof TC, Kavalali ET (2007) Differential effects of SNAP-25 deletion on Ca2+—dependent and Ca2+—independent neurotransmission. J Neurophysiol 98(2):794–806. https://doi.org/10.1152/jn.00226.2007

Chen YA, Scheller RH (2001) SNARE-mediated membrane fusion. Nat Rev Mol Cell Biol 2(2):98–106. https://doi.org/10.1038/35052017

Delgado-Martinez I, Nehring RB, Sorensen JB (2007) Differential abilities of SNAP-25 homologs to support neuronal function. J Neurosci 27(35):9380–9391. https://doi.org/10.1523/JNEUROSCI.5092-06.2007

Duc C, Catsicas S (1995) Ultrastructural localization of SNAP-25 within the rat spinal cord and peripheral nervous system. J Comp Neurol 356(1):152–163. https://doi.org/10.1002/cne.903560111

Fossati G, Morini R, Corradini I, Antonucci F, Trepte P, Edry E, Sharma V, Papale A, Pozzi D, Defilippi P, Meier JC, Brambilla R, Turco E, Rosenblum K, Wanker EE, Ziv NE, Menna E, Matteoli M (2015) Reduced SNAP-25 increases PSD-95 mobility and impairs spine morphogenesis. Cell Death Differ 22(9):1425–1436. https://doi.org/10.1038/cdd.2014.227

Garbelli R, Inverardi F, Medici V, Amadeo A, Verderio C, Matteoli M, Frassoni C (2008) Heterogeneous expression of SNAP-25 in rat and human brain. J Comp Neurol 506(3):373–386. https://doi.org/10.1002/cne.21505

Gu Y, Huganir RL (2016) Identification of the SNARE complex mediating the exocytosis of NMDA receptors. Proc Natl Acad Sci USA 113(43):12280–12285. https://doi.org/10.1073/pnas.1614042113

Hagiwara A, Fukazawa Y, Deguchi-Tawarada M, Ohtsuka T, Shigemoto R (2005) Differential distribution of release-related proteins in the hippocampal CA3 area as revealed by freeze-fracture replica labeling. J Comp Neurol 489(2):195–216. https://doi.org/10.1002/cne.20633

Haglerød C, Kapic A, Boulland JL, Hussain S, Holen T, Skare O, Laake P, Ottersen OP, Haug FM, Davanger S (2009) Protein interacting with C kinase 1 (PICK1) and GluR2 are associated with

presynaptic plasma membrane and vesicles in hippocampal excitatory synapses. Neuroscience 158(1):242–252
Hohenstein AC, Roche PA (2001) SNAP-29 is a promiscuous syntaxin-binding SNARE. Biochem Biophys Res Commun 285(2):167–171. https://doi.org/10.1006/bbrc.2001.5141
Holderith N, Lorincz A, Katona G, Rozsa B, Kulik A, Watanabe M, Nusser Z (2012) Release probability of hippocampal glutamatergic terminals scales with the size of the active zone. Nat Neurosci 15(7):988–997. https://doi.org/10.1038/nn.3137
Holt M, Varoqueaux F, Wiederhold K, Takamori S, Urlaub H, Fasshauer D, Jahn R (2006) Identification of SNAP-47, a novel Qbc-SNARE with ubiquitous expression. J Biol Chem 281(25):17076–17083. https://doi.org/10.1074/jbc.M513838200
Hussain S, Davanger S (2011) The discovery of the soluble N-ethylmaleimide-sensitive factor attachment protein receptor complex and the molecular regulation of synaptic vesicle transmitter release: the 2010 Kavli prize in neuroscience. Neuroscience. https://doi.org/10.1016/j.neuroscience.2011.05.057
Hussain S, Davanger S (2015) Postsynaptic VAMP/synaptobrevin facilitates differential vesicle trafficking of GluA1 and GluA2 AMPA receptor subunits. PLoS One 10(10):e0140868. https://doi.org/10.1371/journal.pone.0140868
Hussain S, Ringsevjen H, Egbenya DL, Skjervold TL, Davanger S (2016) SNARE protein syntaxin-1 colocalizes closely with NMDA Receptor subunit NR2B in postsynaptic spines in the hippocampus. Front Mol Neurosci 9:10. https://doi.org/10.3389/fnmol.2016.00010
Hussain S, Egbenya DL, Lai YC, Dosa ZJ, Sorensen JB, Anderson AE, Davanger S (2017) The calcium sensor synaptotagmin 1 is expressed and regulated in hippocampal postsynaptic spines. Hippocampus. https://doi.org/10.1002/hipo.22761
Jurado S, Goswami D, Zhang Y, Molina AJ, Sudhof TC, Malenka RC (2013) LTP requires a unique postsynaptic SNARE fusion machinery. Neuron 77(3):542–558. https://doi.org/10.1016/j.neuron.2012.11.029
Kerti K, Lorincz A, Nusser Z (2012) Unique somato-dendritic distribution pattern of Kv4.2 channels on hippocampal CA1 pyramidal cells. Eur J Neurosci 35(1):66–75. https://doi.org/10.1111/j.1460-9568.2011.07907.x
Lau CG, Takayasu Y, Rodenas-Ruano A, Paternain AV, Lerma J, Bennett MV, Zukin RS (2010) SNAP-25 is a target of protein kinase C phosphorylation critical to NMDA receptor trafficking. J Neurosci 30(1):242–254. https://doi.org/10.1523/JNEUROSCI.4933-08.2010
Malinow R, Malenka RC (2002) AMPA receptor trafficking and synaptic plasticity. Annu Rev Neurosci 25:103–126. https://doi.org/10.1146/annurev.neuro.25.112701.142758
Mandolesi G, Vanni V, Cesa R, Grasselli G, Puglisi F, Cesare P, Strata P (2009) Distribution of the SNAP25 and SNAP23 synaptosomal-associated protein isoforms in rat cerebellar cortex. Neuroscience 164(3):1084–1096. https://doi.org/10.1016/j.neuroscience.2009.08.067
Mathiisen TM, Nagelhus EA, Jouleh B, Torp T, Frydenlund DS, Mylonakou MN, Amiry-Moghaddam M, Covolan L, Utvik JK, Riber B, Gujord KM, Knutsen J, Skare Ø, Laake P, Davanger S, Haug FM, Rinvik E, Ottersen OP (2006) Postembedding immunogold cytochemistry of membrane molecules and amino acid transmitters in the central nervous system. In: Zaborszky L, Wouterlood FG, Lanciego JL (eds) Neuroanatomical tract-tracing 3: molecules, neurons, and systems. Springer, New York, pp 72–108
Megias M, Emri Z, Freund TF, Gulyas AI (2001) Total number and distribution of inhibitory and excitatory synapses on hippocampal CA1 pyramidal cells. Neuroscience 102(3):527–540
Ravichandran V, Chawla A, Roche PA (1996) Identification of a novel syntaxin- and synaptobrevin/VAMP-binding protein, SNAP-23, expressed in non-neuronal tissues. J Biol Chem 271(23):13300–13303
Risinger C, Blomqvist AG, Lundell I, Lambertsson A, Nassel D, Pieribone VA, Brodin L, Larhammar D (1993) Evolutionary conservation of synaptosome-associated protein 25 kDa (SNAP-25) shown by Drosophila and Torpedo cDNA clones. J Biol Chem 268(32):24408–24414
Roberts LA, Morris BJ, O'Shaughnessy CT (1998) Involvement of two isoforms of SNAP-25 in the expression of long-term potentiation in the rat hippocampus. Neuroreport 9(1):33–36
Sadoul K, Lang J, Montecucco C, Weller U, Regazzi R, Catsicas S, Wollheim CB, Halban PA (1995) SNAP-25 is expressed in islets of Langerhans and is involved in insulin release. J Cell Biol 128(6):1019–1028
Selak S, Paternain AV, Aller MI, Pico E, Rivera R, Lerma J (2009) A role for SNAP25 in internalization of kainate receptors and synaptic plasticity. Neuron 63(3):357–371. https://doi.org/10.1016/j.neuron.2009.07.017
Stuchlik A (2014) Dynamic learning and memory, synaptic plasticity and neurogenesis: an update. Front Behav Neurosci 8:106. https://doi.org/10.3389/fnbeh.2014.00106
Tafoya LC, Mameli M, Miyashita T, Guzowski JF, Valenzuela CF, Wilson MC (2006) Expression and function of SNAP-25 as a universal SNARE component in GABAergic neurons. J Neurosci 26(30):7826–7838. https://doi.org/10.1523/JNEUROSCI.1866-06.2006
Takamori S, Holt M, Stenius K, Lemke EA, Gronborg M, Riedel D, Urlaub H, Schenck S, Brugger B, Ringler P, Muller SA, Rammner B, Grater F, Hub JS, De Groot BL, Mieskes G, Moriyama Y, Klingauf J, Grubmuller H, Heuser J, Wieland F, Jahn R (2006) Molecular anatomy of a trafficking organelle. Cell 127(4):831–846. https://doi.org/10.1016/j.cell.2006.10.030
Tao-Cheng JH, Du J, McBain CJ (2000) Snap-25 is polarized to axons and abundant along the axolemma: an immunogold study of intact neurons. J Neurocytol 29(1):67–77
Tomasoni R, Repetto D, Morini R, Elia C, Gardoni F, Di Luca M, Turco E, Defilippi P, Matteoli M (2013) SNAP-25 regulates spine formation through postsynaptic binding to p140Cap. Nat Commun 4:2136. https://doi.org/10.1038/ncomms3136
Walch-Solimena C, Blasi J, Edelmann L, Chapman ER, von Mollard GF, Jahn R (1995) The t-SNAREs syntaxin 1 and SNAP-25 are present on organelles that participate in synaptic vesicle recycling. J Cell Biol 128(4):637–645
Washbourne P, Thompson PM, Carta M, Costa ET, Mathews JR, Lopez-Bendito G, Molnar Z, Becher MW, Valenzuela CF, Partridge LD, Wilson MC (2002) Genetic ablation of the t-SNARE SNAP-25 distinguishes mechanisms of neuroexocytosis. Nat Neurosci 5(1):19–26. https://doi.org/10.1038/nn783